The Astrophysical Journal, 897:60 (10pp), 2020 July 1 https://doi.org/10.3847/1538-4357/ab9533

Cradle(s) of the Sun

Susanne Pfalzner[1,2] and Kirsten Vincke[2]
[1] Jülich Supercomputing Center, Forschungszentrum Jülich, D-52428 Jülich, Germany; s.pfalzner@fz-juelich.de
[2] Max-Planck-Institut für Radioastronomie, Auf dem Hügel 69, D-53121 Bonn, Germany
Received 2020 March 10; revised 2020 April 29; accepted 2020 May 19; published 2020 July 2

Abstract

The Sun likely formed as part of a group of stars. A close stellar flyby by one of the solar siblings is probably responsible for the sharp outer edge in the solar system's mass distribution. The frequency of such close flybys can be used to determine the likely type of birth environment of the solar system. Young stellar groups develop very quickly, expanding significantly within just a few million years. Here we model this strong dynamical development of young stellar groups and determine the resulting close flyby history. We find that solar system equivalents are predominantly produced in areas with stellar densities in the range $5 \times 10^4\,\mathrm{pc}^{-3} < n_{\mathrm{local}} < 2 \times 10^5\,\mathrm{pc}^{-3}$. Remarkably, we find that only two very distinct types of stellar groups can be considered as serious contestants as the cradle of the Sun—high-mass, extended associations ($M_c >$ 20,000 $M_\odot$) and intermediate-mass, compact clusters ($M_c <$ 3000 $M_\odot$). Present-day counterparts would be the association NGC 2244 and the M44 cluster, respectively. In these two types of stellar groups, close flybys take place at a sufficiently high rate, while not being too destructive either. A final decision between these two remaining options will require the incorporation of constraints from cosmochemical studies.

Unified Astronomy Thesaurus concepts: Solar system formation (1530); Young star clusters (1833); Gravitational interaction (669); N-body simulations (1083)

1. Introduction

In recent years, the first solar sibling candidates have been identified (Bobylev & Bajkova 2014; Ramírez et al. 2014; Liu et al. 2016; Martínez-Barbosa et al. 2016; Webb et al. 2020), which strengthens the earlier argument that the Sun was born as part of a group of stars (Adams 2010). There are several properties of the solar system that have been interpreted as indicators of the influence of this stellar group on the forming solar system:

1. The sharp outer edge of the solar system at about 30–35 au;
2. The orbits of trans-Neptunian objects like Sedna, 2012 VP_{113} and 2015 TG387;[3] and
3. The relatively high content of ^{26}Al and ^{60}Fe in chondritic meteorites.

Each of the solar system features has been applied to constrain the properties of the solar system birth cluster (Ida et al. 2000; Kenyon & Bromley 2004; Adams et al. 2006; Spurzem et al. 2009; Owen et al. 2010; Mitchell & Stewart 2011; Jílková et al. 2015; Li & Adams 2015; Dai et al. 2018). In particular, the presence of the short-lived radionuclides ^{60}Fe and/or ^{26}Al were used to estimate the number of stars/mass of the solar birth cluster (Thrane et al. 2006; Dauphas & Chaussidon 2011; Adams et al. 2014; Parker et al. 2014; Lichtenberg et al. 2016; Nicholson & Parker 2017). These calculations assume that these short-lived radionuclides were incorporated after a supernova outburst in the solar birth cluster. Adams (2010) deduced a lower limit of $N > 10^3$ on the number of stars in the solar birth cluster, translating roughly to a cluster mass of $M_c > 500\ M_\odot$. Recently, Portegies Zwart (2019) puts a very specific constraint of $N = 2500 \pm 300$ stars and a radius of $r_{\mathrm{vir}} = 0.75 \pm 0.25$ pc forward on a similar argument. In recent years the requirement of a supernova explosion in the close vicinity of the Sun has been questioned as alternatives for the origin of ^{60}Fe and/or ^{26}Al have been suggested (for example Wasserburg et al. 2006; Gounelle 2015; Fujimoto et al. 2018). However, the debate is still ongoing (Goodson et al. 2016; Boss 2017; Nicholson & Parker 2017; Lugaro et al. 2018), therefore, it is not clear in how far the above limits hold. Interestingly, chemical considerations demanding the presence of strong far-ultraviolet radiation fields similarly require $N > 4000$ (Lee et al. 2008). However, very massive clusters with $N > 10^5$ have been excluded as solar birth clusters, because the correspondingly large number of very high-mass stars would produce too strong a radiation field (Hester et al. 2004; Williams & Gaidos 2007).

Based on flyby simulations considering the eccentricity and inclination increase of the giant planets, Li & Adams (2015) constrained the upper value of the membership to $N < 10{,}000$ assuming that the stellar birth group was a long-lived cluster. Similarly, Brasser et al. (2006) used Sedna's orbit to provide a lower limit on the central cluster densities of $\rho_{\mathrm{central}} > 10^3\,M_\odot\,\mathrm{pc}^{-3}$, whereas Schwamb et al. (2010) put an upper limit at $10^5\,M_\odot\,\mathrm{pc}^{-3}$. They also assumed that the stellar birth group was a long-lived cluster. Similarly, the orbits of the extreme trans-Neptunian orbits (TNOs; Kenyon & Bromley 2004; Kobayashi et al. 2005; Jílková et al. 2015; Pfalzner et al. 2018b) have been discussed in the context of the solar birth cluster.

These previous investigations mostly took the properties of specific young observed stellar groups, often the Orion Nebula Cluster (ONC), as guidance for their cluster model. It is down to the very nature of observations that they present only a snapshot in time. Therefore most previous simulations tried to

[3] This group of objects is in the following referred to as Sednoids.

reproduce the properties in a quasi-static manner. However, this treatment can only answer the question of whether a stellar group is currently producing solar system analogs, but not what happened in the past or future.

Recently, it has become increasingly clear that young stellar groups are highly dynamical and expand considerably in size during the first 5–10 Myr of their existence (Pfalzner 2009; Kuhn et al. 2019). Another finding, important in this context, is that young stellar groups come in two fairly distinct classes, often referred to as clusters and associations. These two groups show distinctively different expansion histories during the first 10 Myr of their development (Pfalzner 2009; Portegies Zwart et al. 2010). As we will see, this renders a limitation of the solar birth environment in terms of the number of stars alone less meaningful.

The surrounding group of stars could have influenced the solar system either by gravitational interactions with, or radiation from, the other stars. The radiation consists of large amounts of EUV and far-UV (FUV) radiation arising mainly from the massive stars (Adams et al. 2006; Winter et al. 2018) along with X-rays from more distributed sources within the cluster. Together they heat the disk which can eventually lead to its evaporation. For low-mass stars ($\sim$0.5 $M_{\odot}$) in the solar neighborhood, external photoevaporation potentially destroys many of the disks surrounding them (Winter et al. 2020). However, Winter et al. (2020) also find that for solar-type stars ($M \sim 1\ M_{\odot}$) the situation is completely different, in that they are much less affected by external FUV photons. Therefore, although these radiative effects might nevertheless be important in other environments, they are largely beyond the scope of this present work. Here we concentrate on the gravitational effects within the solar birth cluster, however we discuss this limitation in Section 4.2.

The relative importance of the expansion history of clusters and associations in the context of the solar system birth environment was first considered in Pfalzner (2013), which favored massive associations as the solar birth environment. However, our previous study considered only very massive stellar groups (>10,000 $M_{\odot}$), and the expansion phase of clusters was only treated by fitting the observed the cluster sizes as a function of cluster ages and all flybys were approximated as coplanar. Here we take advantage of the recent observational and numerical progress in the understanding of early cluster/association development to update our investigation of the solar birth environment. We thrive for a better representation of the real situation by including noncoplanar flybys, modeling the physical effects that lead to the temporal development of clusters/associations, performing the simulations for a larger range of cluster/association masses, and modeling the embedded, expansion, and semiequilibrium phase of the cluster development self-consistently.

In Section 2 we describe the numerical method including the initial conditions, the dynamics for the different cluster/association models (Section 2.1) and the determination of the effect of flybys (Section 2.2). The results concerning the probabilities of the solar system forming in the various environments are presented in Sections 3 and 4. In Section 5 these results are compared to previous work and implications for future research are outlined.

2. Method

A two-step approach is applied, where first the dynamics of young clusters and associations are modeled, while recording the close flyby history of each star. In a second step, this history is used to determine the flybys leading to a solar-system-like cutoff at 30–50 au of the outer disk.

2.1. Cluster Simulations

The results presented here are based on an extensive set of simulations of the dynamics of different young clusters and associations (Vincke & Pfalzner 2016, 2018; Pfalzner et al. 2018a). In these works we used the code Nbody6++GPU (Aarseth 2003; Wang et al. 2015) to simulate the stellar dynamics of various types of clusters/associations. The model parameters (see Table 1) are chosen to match the observed cluster and association properties including the temporal development of both groups (Pfalzner & Kaczmarek 2013). For each model observational equivalents are indicated: models A1–A3/A4 can be understood as representative of Mon R2, the ONC, and NGC 2244 or NGC 6611, respectively, whereas C1 and C2/C3 roughly correspond to younger counterparts of the clusters Praeceps and Westerlund 2 or NGC 3603. The parameters of models C2 and C3, and A3 and A4 are identical apart from the duration of the embedded phase. The parameters of the various stellar groups are not chosen to be perfect matches to these specific clusters, but we model specific characteristic stellar environments. To aid connecting those to real observed clusters we name stellar groups that can be seen as representatives for the specific group of similar environments. The idealization used for our model clusters is discussed in more detail in Section 4.4.

Starting at the end of the star formation process,[4] the stellar group is still embedded in the gas, which is modeled as a background potential. The cluster half-mass radii of 0.2 and 1.3 pc, respectively, correspond to those typically observed at the start of the expansion phase (Pfalzner & Kaczmarek 2013) for the two types of stellar groups. Equally the star formation efficiencies (SFEs) correspond to those typically observed in associations (0.3) (Lada & Lada 2003) and clusters (0.7) (Rochau et al. 2010; Cottaar et al. 2012; Hénault-Brunet et al. 2012; Krause et al. 2016). The stellar density distribution is modeled as a modified King profile for the stars and a corresponding Plummer profile for the gas which reflects the situation in observed clusters (Espinoza et al. 2009; Steinhausen & Pfalzner 2014). The two profiles have the same half-mass radius meaning that the Plummer core radius is given as $r_c = r_{\rm hm}/1.305$ (Plummer 1911). The stellar masses were sampled from an initial mass function (Kroupa 2002) with a lower limit of 0.08 and an upper limit of 150. We assume the clusters to be initially in virial equilibrium and chose the velocities following the corresponding Maxwellian distribution.

The development of the gas component at the end of the star formation process is complex and would require detailed knowledge of the gas dispersal mechanism. Given the lack of this knowledge, we make the simplifying assumption that the gas distribution roughly follows the stellar distribution, but is somewhat flatter in the central area. The latter being motivated by the fact that, for example, the ONC is nearly gas-free in its

[4] This means that the times given are not necessarily equivalent to the cluster age as the star formation phase is not covered.

Table 1
Setup Parameters of the Modeled Associations and Clusters

Model	N_{stars}	N_{sim}	SFE	r_{hm}	t_{emb}	t_{dyn}	Type	Represents
				(pc)	(Myr)			
A1	1000	308	0.3	1.3	2.0	0.67	A	Mon R2
A2	4000	94	0.3	1.3	2.0	0.33	A	ONC
A3	32,000	9	0.3	1.3	2.0	0.12	A	NGC 2244, NGC 6611
A4	32,000	9	0.3	1.3	1.0	0.12	A	NGC 2244, NGC 6611
C1	4000	50	0.7	0.2	1.0	0.03	C	M44
C2	32,000	10	0.7	0.2	1.0	0.01	C	NGC 3603, Westerlund 2
C3	32,000	10	0.7	0.2	0.0	0.01	C	NGC 3603 Westerlund 2

Note. Column (1) gives the model name, N_{stars} (2) is the number of stars in the model, N_{sim} (3) is the number of simulations in the simulation campaign, SFE (4) is the star formation efficiency, r_{hm} (5) is the initial half-mass radius of the stellar and the gas component, t_{emb} (6) is the duration of the embedded phase, (7) indicates the dynamical timescale, (8) gives the type of stellar group, where A stands for association and C for cluster, and (9) represents a cluster that roughly serves as a young equivalent.

center. A Plummer profile fulfills this requirement of being flatter in the center than the King profile applied for the stars. Using a Plummer profile for the gas has the additional advantage that it has a fixed outer edge, whereas King profiles do not.

The gas is expelled instantaneously at the times t_{emb} specified in Table 1. Assuming such instantaneous gas expulsion is justified as in all considered cases $t_{gas} < t_{emb} < 1$ Myr. As we will see, the effect of gas expulsion is less pronounced for clusters than for associations due to the difference in SFE. For associations, gas expulsion is the main reason for cluster expansion and up to 90% of stars become unbound. Clusters also expand despite their high SFE, however, the underlying reason is the high number of stars ejected from the densest central cluster regions (Pfalzner & Kaczmarek 2013) rather than being the effect of gas expulsion.

Tracking the equivalent of approximately 500,000 stars is required to guarantee that the error in the average disk size is smaller than 3%. In order to fulfill this requirement we perform a considerably larger number of runs, N_{sim}, for each cluster model than is usual. Only for the dense clusters C2 and C3 do we perform fewer runs, because the number of interactions make these simulations computationally expensive. The individual simulations are combined by determining the respective properties in the individual simulations and calculating their mean value.

Binaries were not included in the initial setup, but were correctly tracked when formed by capturing events. This choice was motivated by the fact that parameter space for the flybys would increase dramatically for binaries. However, this point should be investigated in detail in future studies.

2.2. Effect of a Flyby on the Disk Size

In the postprocessing step the recorded close flyby history is used (periastron distance, r_{peri}, and the mass ratio of encounter partners, $m_{12} = m_2/m_1$) to determine the effect on the disks. Here m_2 denotes the mass of the perturber star and m_1 the mass of the central star. Each star is treated as initially being surrounded by a 200 au sized disk. Here, the actual initial size is of minor importance, as long as it is significantly larger than the 30–50 au tested for. The disk size for every solar-type star after a flyby, R_d, is determined based on the parameter studies by Breslau et al. (2014) and Bhandare et al. (2016). The simulation results of these two studies can be approximated by simple functions of the form

$$R_d = 1.6 \cdot r_{peri}^{0.72} \cdot m_{21}^{-0.2}, \quad (1)$$

where r_d and r_{peri} are given in astronomical units and $m_{21} = m_2/m_1$ is the ratio between the masses of the perturber star (m_2) to that of the host star (m_1). For the solar system $m_1 = 1\,M_\odot$ therefore this simplifies to

$$R_d = 1.6 \cdot r_{peri}^{0.72} \cdot m_2^{-0.2}. \quad (2)$$

The disk sizes given are those averaged over all possible inclinations for such a flyby. Previous studies were often restricted to flybys between coplanar orbits (e.g., Pfalzner 2013; Portegies Zwart & Jílková 2015; Vincke et al. 2015). As such the values given here are more realistic because they take the inclination between the stars into account.

We define stars that have masses between 0.8 and 1.2 $M_\odot$ as solar-type stars. These constitute roughly 5% of the stellar population in the stellar groups modeled here. Among those stars we search for flybys that lead to a postflyby disk in the range 30–50 au. In the following, these are referred to as solar system analogs (SSAs). Equation (2) shows that flybys have to be very close to lead to such disk sizes unless the perturbing star is of relatively high mass. For example, for an encounter with an equal mass star, $m_2 = 1$, the periastron distance has to be of the order of 50–80 au. By contrast, a 50 $M_\odot$ star would have the same effect passing at a distance of 110–175 au.

While using Equation (2) now includes inclined flybys, it is still restricted to parabolic orbits. Including the eccentricity would mean extending the already extensive parameter space by at least an additional factor of ten. Instead, we record the eccentricity in the cluster simulations so that we can see in which cases this approximation is justified and where it fails. We will discuss in Section 4 in how far this approximation influences the obtained results.

Besides, viscous spreading after flybys is neglected, meaning disk sizes can only become smaller by consecutive close flybys. If the disk still contains significant amounts of gas, viscous

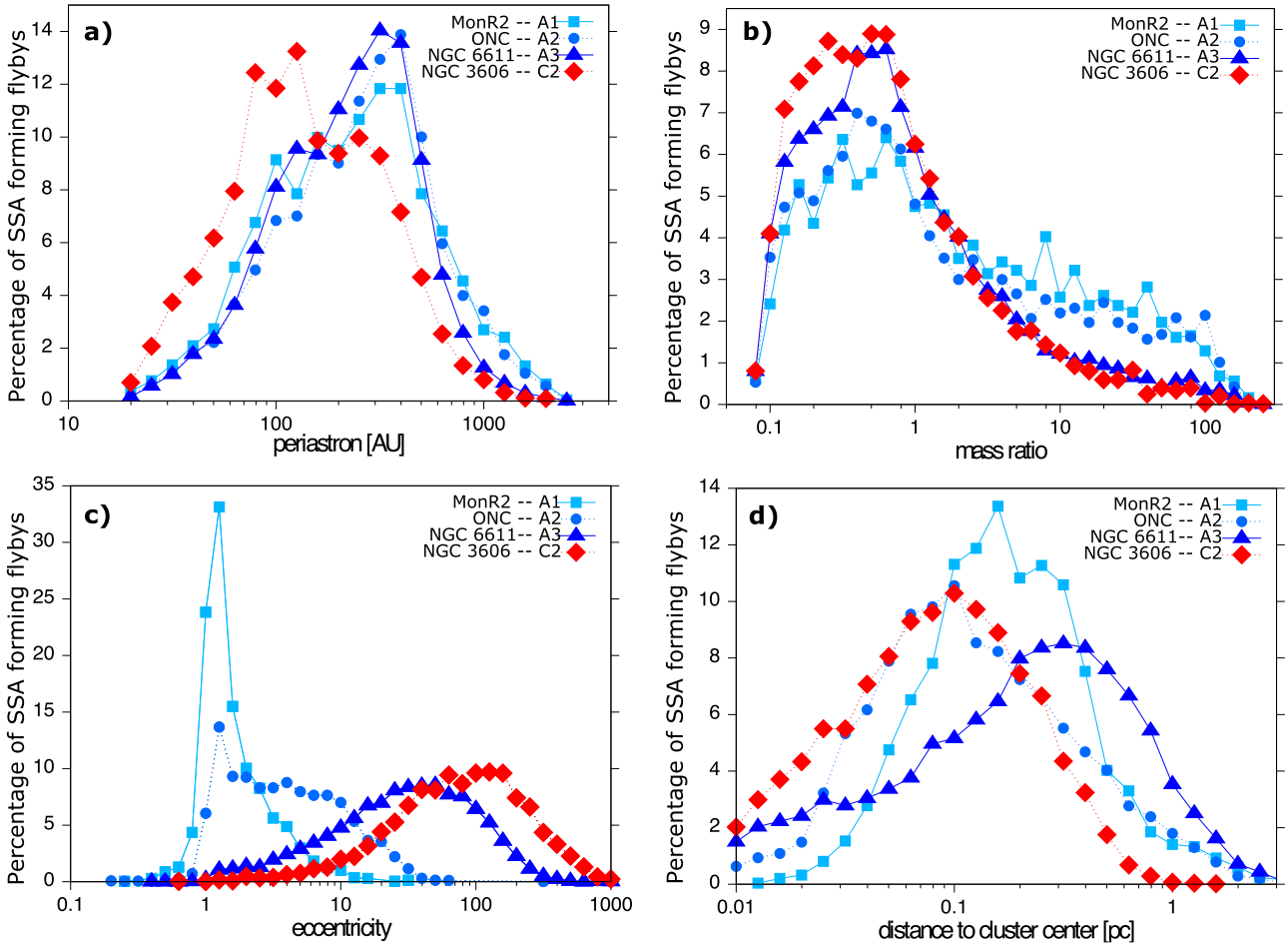

Figure 1. Here only solar-type stars ($0.8 < m_1 < 1.2$) are considered that have solar-system-sized disks at the end of the simulation. Shown are the percentage of stars where the solar-system-forming flyby had a specific property value. The parameters shown are (a) the periastron distance, (b) the mass ratio, (c) the eccentricities, and (d) the distance to the cluster center.

effects can lead to an increase in disk size over time (Cuello et al. 2019). This process tends to smear out the outer disks' edges. However, in the case of the solar system we deal with a sharp outer edge. Thus, the flyby must have occurred either just shortly before or after gas dispersal from the disk, or it had a very low viscosity. Thus a purely gravitational treatment seems to suffice here.

There is a slight inconsistency in our treatment as we do not take into account the matter captured from the perturber star. However, the captured matter usually moves on extremely eccentric orbits with short periastron distances (Pfalzner et al. 2005), and as such it does not significantly contribute to the disk size. It also might constitute an important part in the TNO population (Pfalzner et al. 2018b).

3. Results

First, we want to have a look at the properties of the flybys that lead to SSAs. Only SSAs are considered, meaning stars with masses between 0.8 and 1.2 $M_\odot$ and postflyby disks in the range 30–50 au are at the end of the simulation. Figure 1 shows the percentage of stars that underwent a flyby with the respective properties: (a) periastron distances, (b) mass ratios, (c) eccentricities, and (d) distances to the cluster center of SSAs averaged over all simulations for models A1–A3 and C2, representative for clusters like Mon R2, ONC, NGC 6611, and NGC 3603, respectively. Models A4, C1, and C3 have been omitted, as they follow similar trends to A3 and C2. In a naive approach, one would expect that the distribution of periastron distances that lead to a 30–50 au sized disk is independent of cluster environments. This is valid for the association models (A1–A3), however in massive dense clusters (illustrated here for model C2) the SSA-forming flybys are on average closer with a maximum at 90 au.

Figure 1(b) gives some insight into the reason for this difference between clusters and associations. It shows the distribution of the masses of the perturbers that lead to SSAs. While in all four shown cases the maximum of the distribution lies below 1, for models A1 and A2 (blue and turquoise lines) a considerable proportion of perturbers have very high masses ($>10\ M_\odot$). As a result, the perturbers tend to have on average higher mass in the associations than in clusters (red line). The reason is that in associations the massive stars function as gravitational focuses for the low-mass stars in these comparably low-density environments, and are largely responsible for the truncation of disks around low-mass stars. By contrast, in very compact clusters the stellar density is so high that the massive stars lose their dominant role because close flybys between low-mass stars become so common that gravitational focusing does not play such an important role anymore. The most massive stars are "shielded" by the high density of lower stars surrounding them. This means that here it is the equal mass encounters that dominate the production of SSAs. Model

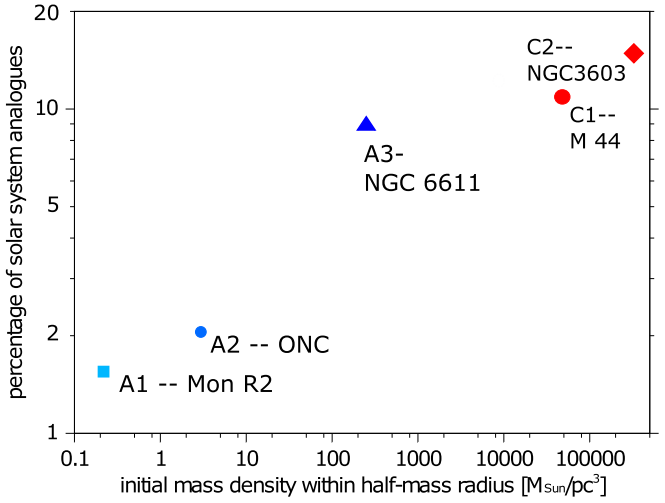

Figure 2. Percentage of SSAs as a function of initial cluster density. Values are given for the time at the end of the simulation run.

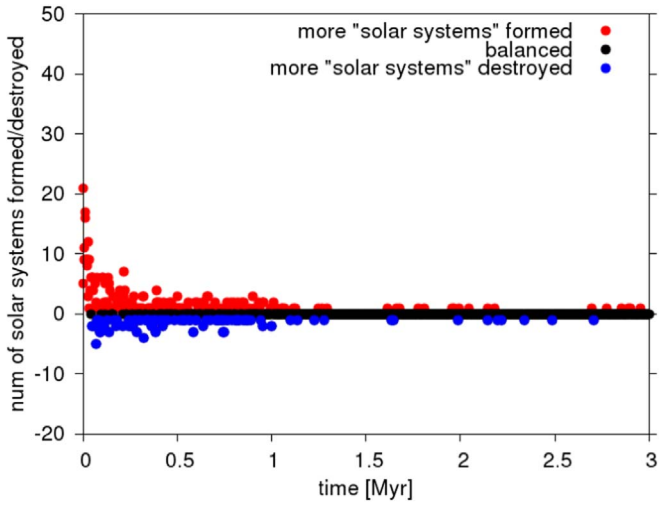

Figure 3. Number of disks truncated to SSAs (red) within a time interval of 0.01 Myr as a function of time, and the number of SSAs truncated during that period to even smaller sizes, meaning they are too small to form an SSA (blue). Here the case for model C2 is shown.

A3 is basically at an in-between state because in the central areas the density is comparable to that in clusters but at the outskirts, it is more like lower-mass associations.

This interpretation is strongly supported by Figure 1(c), which shows the eccentricity distribution of SSA-forming flybys. For the lowest density associations, all flybys are on parabolic orbits ($e = 1$), whereas for high-mass clusters the flybys show high eccentricities—a similar behavior was already noted in Olczak et al. (2012). However, hyperbolic flybys are expected to have a weaker influence on the disk (see, e.g., Pfalzner 2004; Winter et al. 2018). As we use the approximation of parabolic flybys in Equation (2), we will discuss the consequences of this approximation on the results in Section 4.1.

Figure 1(d) shows the location of SSAs in terms of distance to the cluster center at the end of the simulation. The position of SSAs varies strongly among the different association and cluster models and the explanation is somewhat more complex. For models A1–A3 the vast majority of SSAs are located within their half-mass radius of 1.3 pc. However, there are considerable differences in the location of the maxima in the distributions. Model A1 reacts slowest to the gas expulsion due to the low stellar density, therefore, most SSA-forming flybys occur around the border to the cluster center (≈0.15 pc). Model A3 is much more dense, therefore it expands quite violently after gas expulsion, while it does not dissolve completely. Therefore the center is so dense that many close flybys lead to overly small systems, therefore, the peak of the distribution is further out at approximately 0.4 pc. Model A2 is between A1 and A3 in terms of density and dynamical reaction time. As a result, most SSAs are very close to the association center at about 0.1 pc or even less. It is pure coincidence that this more or less matches the peak in the distribution for model C1. For model C1 the situation is similar to A3, but more extreme in that most SSAs are located far from the actual center at ≈0.3 pc, this means outside the initial half-mass radius of 0.2 pc. Outside roughly 0.5 pc, the number of SSA flybys becomes negligible. The reason is that the cluster expands comparatively little after gas expulsion because the SFE is so high.

Figure 2 shows the percentage of SSAs at the end of the respective simulation runs as a function of cluster density. Here density is defined as the initial mass density (stars+gas) within the initial half-mass radius (1.3 pc for associations, 0.2 pc for the cluster). In A1, but even the denser A2, the relative number of systems that are reduced to solar system sizes is relatively low, only 1%–2% of the disks are SSAs. The latter value is in agreement with earlier studies in these environments (Adams 2010).

As expected, the proportion of SSAs increases with density, and in much denser associations, like A3/A4, approximately 9%–11% of systems within the half-mass radius are SSAs. In compact clusters like C2, the portion increases even more to about 13%–17% of stars, depending on model parameters. However, it would be premature to conclude that clusters like C2 or even denser clusters are the most likely environment for the solar system to have formed in. Figure 3 shows the number of events per timestep of disks being reduced to SSA size (red circles) and those that are truncated below 30 au (blue circles) as a function of time for the example of C2. With $R_d > 30$ au, the latter systems are too small to form SSAs. In the initial stages ($\ll$0.1 Myr) the number of SSA-forming events dominates over the destruction events, however, after just a short time the situation is reversed and there are many more SSA destruction events than formation events.

C2 is so dense that truncation to SSA size is readily achieved; here the problem is that the systems tend to become very small. This can be seen better in the distribution of disk sizes given in Figure 4. Here the distribution is depicted at the end of the simulation runs for A1, A2, A3, and C2. It can be seen that for the associations, the disks larger than the solar system are always dominant.

In model A2 approximately 85% of disks around solar-type stars are larger than 100 au, whereas roughly 5% are smaller than 30 au and only ≈1.8% are solar-system-sized at an age of 10 Myr. In the less dense model A1, only ≈1.2% of the systems resemble the solar system, while ≈95% are larger than 100 au. The situation is different in the very massive association A3, where roughly 7%–10% of disks are SSAs and only ≈50% are larger than 100 au.

The disk-size distribution differs completely in dense clusters, where the average disk size is well below 20 au (Vincke & Pfalzner 2018). Consequently, most disks (≈66%)

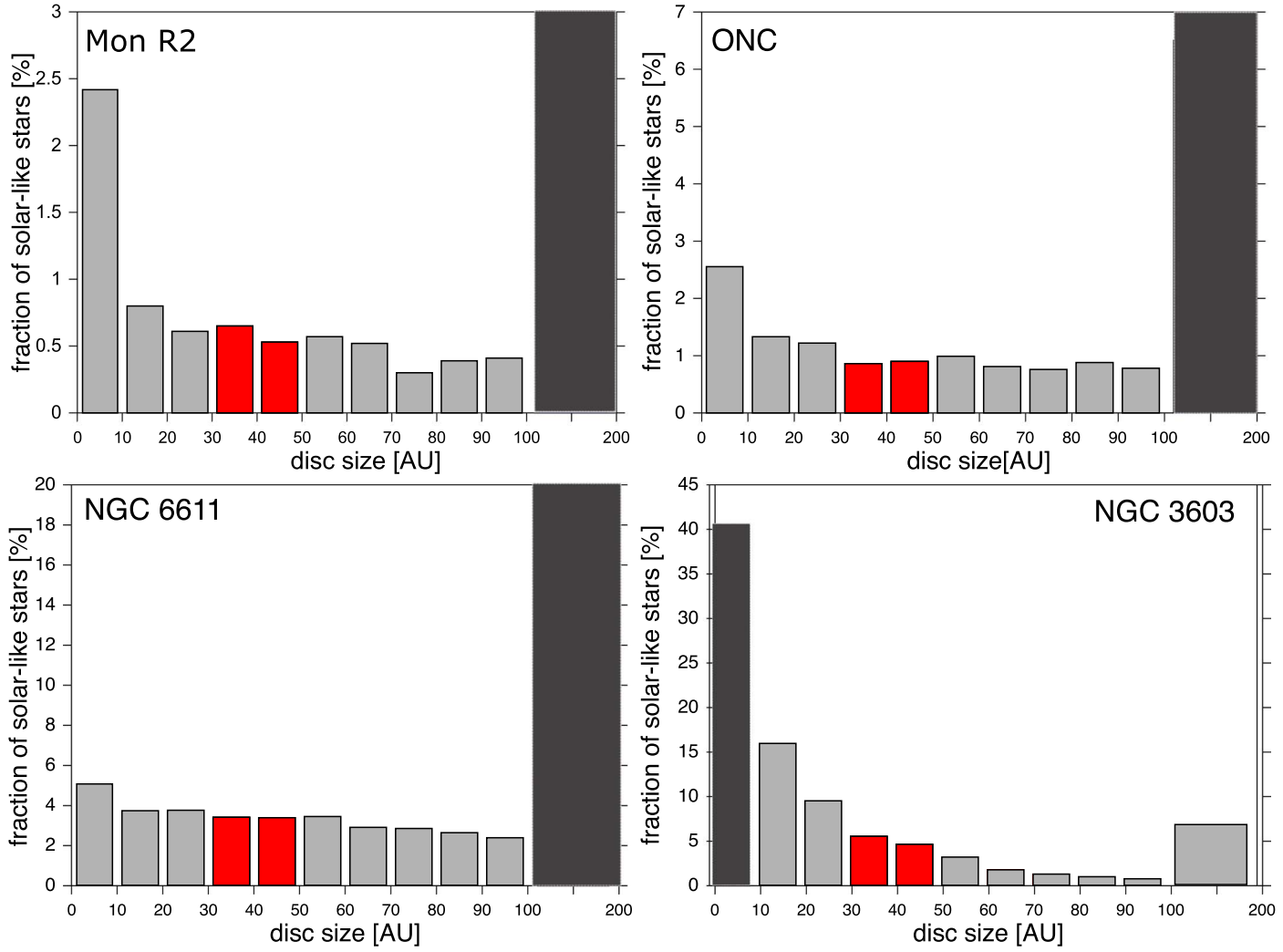

Figure 4. System size distribution of simulated clusters A1, A2, A3, and C2, representative of Mon R2, ONC, NGC 6611, and NGC 3603. The red bars highlight the system sizes similar to the solar system, whereas dark gray indicates the most common disk size in the respective clusters. Note that the last bin contains all disks having final sizes between 100 au $\leqslant r_{\rm disk} <$ 200 au. The fractions shown are those for solar-type stars, meaning those in the mass range 0.8 $M_{\odot} < m_1 < 1.2\,M_{\odot}$.

are too small to form SSAs. Many of them (40%) are <10 au implying that they contain so little mass that only very small planetary systems can form, if at all. Nevertheless, ∼15% of all solar-like stars are surrounded by SSAs.

In absolute numbers, SSAs in "small" associations are rare. In A1 environments on average less than one, and in A2-like associations approximately four, SSAs can be expected. The number of SSAs increases significantly in very massive associations, with roughly 100–150 SSAs in A3 environments. For clusters like C2, it is even larger at about 150–250 SSAs.

However, these 15% or 150–250 SSAs for C2 type clusters are representative only for $t = 3$ Myr. Figure 5 shows that the actual percentage of SSAs decreases on longer timescales. This effect is most pronounced in dense clusters. For model C3, a large proportion of the disks are already truncated to solar system sizes (≈50%) within the first 0.01 Myr. Afterwards, disks still experience SSA-forming flybys, however, an even larger number are "destroyed," i.e., truncated to $r_{\rm disk} < 30$ au. In summary, this leads to a constant decrease in SSAs. The situation is only slightly different when one considers a longer embedded phase (model C1). Here the different velocity distribution leads initially to slightly more SSAs as flybys that truncate the disks below 30 au are somewhat rarer. However, this is canceled out when gas expulsion happens, so that at 3 Myr the number of SSAs is nearly the same.

This decrease in the number of SSAs over time also happens in systems A1–A3. However, the decline in the number of SSAs is always much slower than in clusters due to the lower density. It might be surprising that an overall decline does take place in these environments, but the stars that encounter close flybys are usually located close to the cluster center and often remain there, so the probability for a consecutive close flyby is higher for SSAs than for the population as a whole.

This means that in dense clusters the problem is not that close flybys are rare but, in contrast, that they are so common. Disks are often truncated to smaller sizes than the solar system. As the cluster density changes very little after 3 Myr, one can extrapolate this behavior. At about 35 Myr the number of SSAs in such dense clusters is lower in C2 than in A3, and by then disk truncation to sizes <30 au will have reduced the proportion of SSAs to less than 10%. This destruction of SSAs carries on until the clusters dissolve. As a consequence, it is more likely that the solar system formed in a smaller-mass cluster or a relatively high-mass association, like A3, than in a dense cluster like C2.

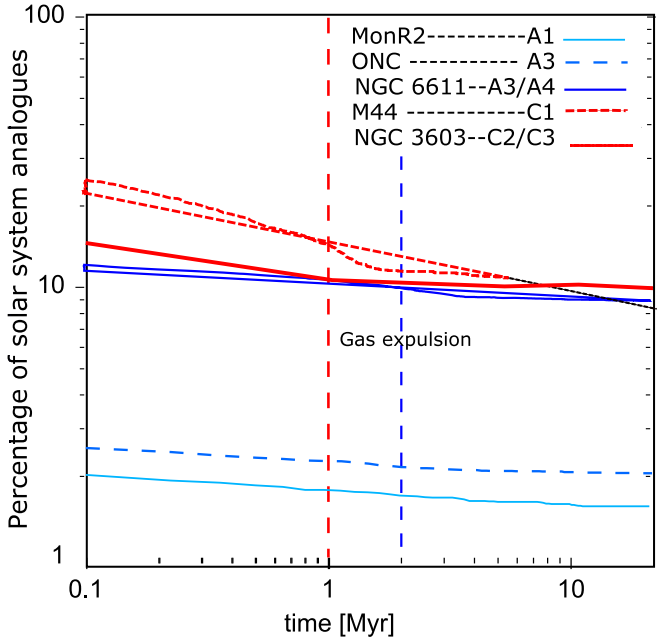

Figure 5. Number of solar-system-sized disks as a function of time for models A1-Taurus, A2-ONC, C1-M44, A3-NGC 6611, and C2-NGC 3603. Where there are two lines in the same line style, the models with a short and long embedded phase are both shown. The vertical lines indicate the time of gas expulsion as given in Table 1.

4. Limitations

Two factors might influence our results, namely, the assumption of parabolic flybys and the restriction to gravitational interactions only. In the following we will discuss their possible effects.

4.1. Parabolic Flybys

The above simulations assumed that all flybys were parabolic. As Figure 1(b) illustrates, this is valid for Taurus-like stellar groups and also to some degree for ONC-like ones, so that our results should still hold here. However, the situation is different for NGC 6611, M44, and NGC 3603, where most SSA-forming flybys seem to happen on highly eccentric paths. The simplest solution seems to be to treat the flybys as hyperbolic. Olczak et al. (2012) showed that hyperbolic flybys are usually less efficient in removing matter from the disk, resulting in less mass loss and larger disk sizes. If this were the case, then for NGC 6611 and M44 assuming parabolic flybys probably overestimates the SSA-forming events to some degree, and for NGC 3603 the situation is different because here the main hindrance for forming SSAs is that many disks are cut to smaller sizes. Therefore, the number of SSA-forming destroying events here might be overestimated. This could make a particular difference on the timescale of hundreds of millions to billions of years.

However, there is a problem in diagnosing the flyby paths in very dense systems. It is implicitly assumed that, if no capturing process is taking place, the path is parabolic or hyperbolic and can be determined using three points of the orbit. This is valid if the problem can be approximated as a two-body problem and is a reasonably good approximation, as long as the other stars of the cluster can be seen as a perturbance to the two-body problem. However, in the very high-density regions, the actual orbit is neither parabolic nor hyperbolic, instead, the eccentricity of the orbit is constantly changing due to interactions with near neighbors. In this case, a three-point fit with the points being chosen before, at and after periastron passage, gives a fairly arbitrary value, as the property "eccentricity" becomes increasingly meaningless. Therefore in these type of environments, a direct modeling of the effect of the disks would be the best approach. Unfortunately, these are the environments that are currently still not computationally accessible for such massive clusters.

4.2. External Photoevaporation

The proplyds in the center of the ONC show that external photoevaporation can also reduce the sizes of disks (O'dell & Wen 1994; Ricci et al. 2008). In this study we did not include the effect of external photoevaporation, mainly because there is a large uncertainty on the mass-loss rates and their temporal development, and therefore on the timescales on which external photoevaporation acts. Unfortunately, observation of the current mass-loss rate in proplyds does not really resolve the issue. If these proplyds in the core of the ONC would have had the current mass-loss rate over the age of the ONC (Johnstone et al. 1998; Henney et al. 2002; O'Dell et al. 2015), they should be destroyed by now, while in reality 80% of stars are still surrounded by disks (Winter et al. 2019). This is sometimes referred to as "proplyd lifetime problem." Unlike for flybys, the overall effectiveness of photoevaporation seems to depend on parameters which so far are not well constrained.

An important point in this context is that gravitational interactions and external photoevaporation differ in the timing of their peak efficiency. Flybys are most efficient during cluster formation. In contrast, external photoevaporation is least efficient during that period as the gas–dust density is so high that radiation is not very effective at penetrating it. As gas–dust density decreases, external photoevaporation becomes increasingly important, reaching its peak when gas expulsion sets in in the central regions of the stellar group. The ONC proplyds are an illustrative example of this phase. However, this phase where photoevaporation is efficient lasts only for 1–2 Myr, afterwards the stellar density is too low due to the expansion as a reaction to gas expulsion. This sequence of events means that flybys set the scene in terms of disk sizes before photoevaporation sets in.

The question is in how far do we expect external photoevaporation to affect our results. Photoevaporation is probably inefficient in Taurus-like environments as here both the stellar density and the number of massive stars is low. Therefore, the effect on the number of SSAs is probably negligible. In ONC-like stellar groups, photoevaporation does truncate disks, but only in the center of the clusters and only for a relatively short period. During the very early stages, the gas–dust density of the environment is so high that radiation is largely blocked and photoevaporation is ineffective. At later stages and in particular when the central area starts to becomes exposed during the gas-expulsion process, photoevaporation can lead to the truncation of disks around stars that have massive stars in their neighborhood. However, as soon as cluster expansion starts to set in at around 1 Myr, the association expands and external photoionization becomes inefficient.

The situation is quite different in clusters as they are much more compact and, although they expand over the first 5 Myr, most of their stars are still situated typically within just a few

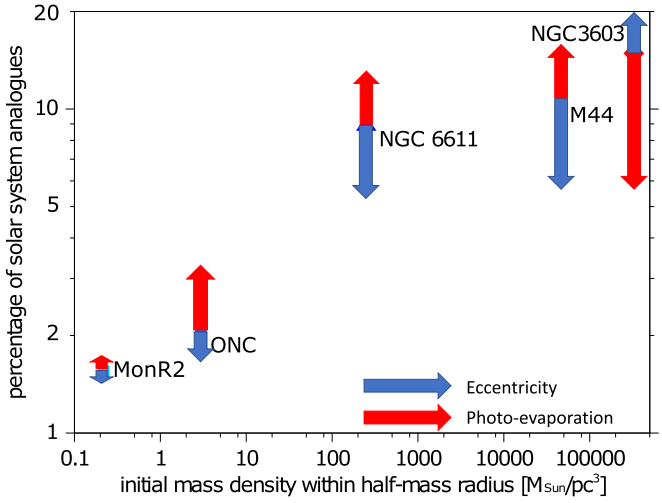

Figure 6. Same as Figure 2 but indicating the potential influence of external photoevaporation and eccentricity of the orbits on the percentage of SSAs for models A1, A2, A3, and C2.

parsecs of each other and remain bound. This means photoevaporation is probably at work for much longer in such an environment. For our densest cluster, NGC 3603, photoevaporation is likely to decrease the number of SSAs, as even more systems will be truncated to very small disk sizes. The situation is less obvious for M44, where the lower density means that photoevaporation could reduce large disks into SSAs, but also truncate SSAs, making even them too small.

Figure 6 tries to capture the situation including the above-discussed uncertainties. In summary, even considering the possibly effects of flybys and photoevaporation, it is most likely that the solar system formed in a relatively high-mass association or a lower-mass cluster. Only if the effect of hyperbolic encounters dominated over that of photoevaporation would there be a realistic chance that the solar system formed in a massive cluster like NGC 3603, Trumpler 14, or Westerlund 2.

4.3. Initial Disk Size

We started out with the somewhat artificial assumption that all disks initially had a size of 200 au. In reality, there will be a distribution of disk sizes. The actual distribution of disk sizes is not well constrained observationally, especially for the embedded phase relevant here. However, it is probably realistic to expect that some stars are surrounded by 30–50 au sized disks at the time our simulation starts.

One could argue that if the percentage of 30–50 au sized disks would be sufficiently high, such disks would already be viable as SSAs in terms of size and would change the percentage of successful systems. However, Figure 2, for example, should not be interpreted merely as the percentage of stars that would be observed with a certain disk size. There is an important additional requirement to be an SSA, namely that the disk has a sharp outer edge, like is characteristic for the solar system. This sharp outer edge is the main reason why it is assumed that a flyby is responsible for the size of the solar system. Thus there might be 30–50 au sized disks to start with in a real star cluster, however, those would not necessarily be an SSA.

4.4. Stellar Groups

The models of the various stellar groups are idealized in several ways, namely as a smooth centrally concentrated distribution with Maxwellian velocity distributions. Obviously none of the named equivalents fit these assumptions perfectly. Real stellar groups will deviate to different degrees from this idealization, by being substructured and/or elongated, and their velocity distribution might deviate from the equilibrium implied by a Maxwellian distribution. For the compact and/or high-mass stellar groups (models A3/A4 and C1–C3), substructure is quickly erased and a equilibrium situation established on a short timescale (see the dynamical timescales in Table 1). This is confirmed by observations showing that the substructure leftover from the fractal structure of the parent molecular cloud typically vanishes within ∼1 Myr (Jaehnig et al. 2015). For those environments the above simulations should represent the situation in real stellar groups well. The situation is different for the lower-mass associations, as they might still show stronger signs from their formation process. However, neither elongation nor slightly lower velocities should lead to a significantly higher proportion of close flybys. By contrast, subclustering might increase the number of close flybys. However, it will not realistically increase the number of close flybys in Mon R2 or the ONC to such a degree to become comparable to those in NGC 6611, M44, or NGC 3603. In summary, these deviations of real clusters from our idealization should be inconsequential for our main result.

5. Discussion

As mentioned in Section 1, there have been many previous constraints on the number of stars in the stellar birth environment based on different properties of the solar system. However, most did not distinguish between short- and long-lived clusters, and clusters and associations. This limits the comparison that can be provided here. Despite this difficulty, Taurus-like environments are generally regarded as very unlikely environments for the formation of the solar system, which we also confirm in our study. Similarly, our results also agree with previous work that stated that ONC-like stellar groups are only moderately likely to represent the solar system birth environment (Lee et al. 2008; Adams 2010).

On the high mass/number end, we agree with the works by Hester et al. (2004) and Williams & Gaidos (2007) that very massive clusters like Westerlund 2 or Trumpler 14 are unlikely solar birth environments because here the density is so high and the radiation strong. However, an important point is that it is not primarily the high density and strong radiation that make these environments too hostile for the solar system to have developed there, but it is mainly the fact that these high densities are maintained for at least tens of millions of years.

Although these findings agree with our results, we think that the mass or number of stars alone are insufficient as a constraint. One major reason is that short- or long-lived clusters (associations and clusters) exist, so that one obtains different constraints on N depending on which of the two different types of stellar groups one considers. But also distinguishing just between clusters and associations is not the best approach. In Pfalzner (2013) we considered both types of stellar groups, even if it was with a number of approximations (see Section 1). Our more detailed study confirms our earlier result that the close flyby frequency in NGC 6611-type clusters is higher than

in the ONC. Equally, we come to the same conclusion that hardly any disks with solar-system-building potential would survive the initial highly interactive phase in very massive star clusters $M_c > 10^4$. This makes high-mass dense clusters like NGC 3603 unlikely environments for SSAs. However, in Pfalzner (2013) we implicitly generalized this result that holds for high-mass dense clusters like NGC 3603 to clusters in general. Our new study shows that this is not valid. Intermediate-mass compact clusters, similar to younger versions of M44, are actually a viable alternative to high-mass short-lived associations like NGC 6611 as solar birth environments.

As demonstrated, neither cluster mass (the number of stars) nor the type of stellar group alone are good constraints for the solar birth environment. We will see that cluster density serves this purpose better but is also not ideal. Our simulations suggest that a cluster with an average peak cluster density of 100–10^5 pc^{-3} is most favorable for the formation of SSAs. The lower limit agrees with previous estimates by Brasser et al. (2006), however our limit upper limit is higher than that of Schwamb et al. (2010) which used the orbit of Sedna as constraint.

Although more suitable than mass, the mean or central cluster density works only if one assumes that most SSA-forming events happen in the center of clusters. However, the frequency of SSA-forming events depends on the distribution of the stars. For example, stellar groups with Plummer profiles lead to lower close flyby rates than King profiles, equally, subclustering also alters the close flyby frequency. We suggest using the proportion of stars that are located in the region where the stellar density favors SSA-forming events instead.

Our simulations show that SSA-forming events happen in 90% of all cases in areas where the local stellar density $\rho_{\rm local}$ exceeds 5×10^4 pc^{-3}. Similar SSA-destroying events happen mostly where $\rho_{\rm local}$ exceeds 2×10^5 pc^{-3}. Therefore the proportion of stars that are contained in areas with 5×10^4 pc^{-3} $< \rho_{\rm local} < 2 \times 10^5$ pc^{-3} gives a good indication of whether a certain environment is likely to produce many SSAs. Below this density SSA-forming events are infrequent, whereas above this SSA destruction becomes the norm. The advantage of using the local stellar density as a constraint is that these limits can be readily applied to any given distribution of stars. Therefore, it can also be applied to observed stellar groups to determine whether SSA-forming events are likely to currently take place.

Applying these constraints to our various models shows that the SSA-forming flybys happen in completely different areas. Figure 7 shows the proportion of stars that lie in this density band for the different stellar groups during the early phases of the evolution. To account for the different extent of the various stellar groups, the location is shown relative to the initial half-mass radius of the various stellar groups, and for comparison the initial mass density distribution in the cluster is also shown. It can seen that for the ONC only a relatively narrow band close to the center has the appropriate stellar density to produce SSAs. By contrast, the dominant SSA-producing region for NGC 6611–like systems and M44-like systems are not in the very center but at a relatively broad region between 0.2 and 0.5 times the half-mass radius. In stark contrast, most SSAs in high-mass, NGC 3603–like clusters actually happen outside the half-mass radius. This means that only if the solar system formed in the outskirts of such a cluster and became unbound within the first 5 Myr would there have been a chance to survive this harsh environment.

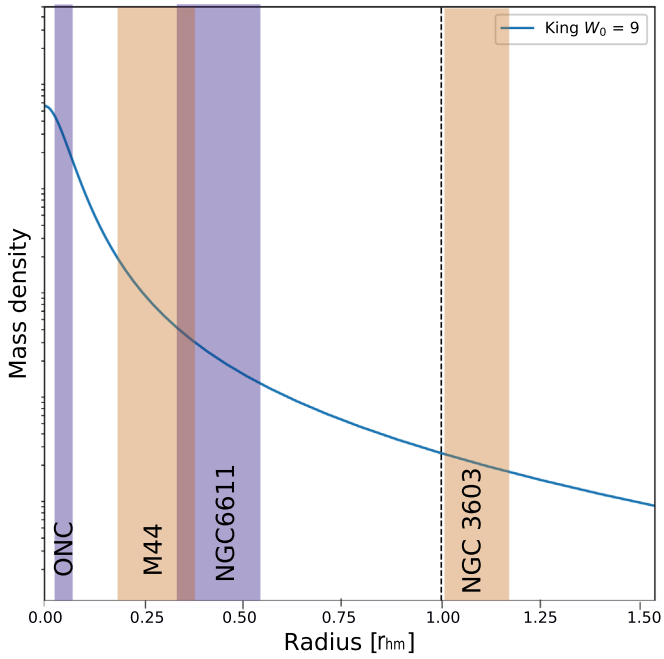

Figure 7. The initial mass density distribution in the cluster models as a function of distance to the cluster center normalized to the half-mass radius. The shaded areas indicate the regions most favorable for SSA production for the different cluster types.

6. Conclusion

Here we have tried to constrain the type of stellar group that provided the birth environment of the solar system. Assuming the sharp outer edge of the solar system was caused by a close stellar flyby, we determined the frequency of SSAs being formed in different types of stellar groups. In contrast to most previous work, we explicitly take the temporal development of such stellar groups into account. Our simulations strongly suggest that the solar system was either born in a massive association ($M_c \approx$ 1–2 $\times 10^4\,M_\odot$) or an intermediate-mass cluster ($M_c \approx$ 1–2 $\times 10^3\,M_\odot$), present-day equivalents being, for example, NGC 6611 and M44 (Praeceps), respectively. In both environments, approximately 10% of solar-type stars experience such a solar-system-forming flyby and the formed system can be expected to remain intact over gigayear timescales afterwards. In future studies, the above specifications of the two types of potential solar birth environments should be complemented by cosmochemical considerations. These could be used to come to a final decision about the solar birth environment.

Whether the Sun formed in a stellar group like the ONC has been previously investigated. We find that the likelihood of solar-system-forming flybys is approximately a factor of five lower in ONC-like associations than in those pinpointed above. The reason is that the peak density in the ONC is a factor of 30–100 lower than in the above detailed environments. Similarly, massive dense clusters ($M_c > 1 \times 10^4\,M_\odot$) also seem to be unsuitable environments for the formation of the Sun. Although initially more SSAs are produced in such clusters, the systems formed are very susceptible to later destruction due to a high encounter frequency. The result is that most planetary systems in such environments can be expected

to be much smaller than 30 au. Only if the Sun formed well outside the half-mass radius of such a cluster and became unbound fairly early on, would it have survived such harsh surroundings.

How can one determine whether a given stellar group is likely to form SSAs? We find that most SSA-forming flybys happen in the early phases at a local stellar density in the range $5 \times 10^4\,\mathrm{pc}^{-3} < n_{\mathrm{local}} < 2 \times 10^5\,\mathrm{pc}^{-3}$. In these environments the stellar density is sufficiently high so as to lead to a high number of close flybys, but also low enough to escape subsequent destruction. Using the proportion of stars located at areas of such stellar densities provides a good constraint for determining the likelihood of forming SSAs. The advantage is that these limits can be readily applied to any given distribution of stars.

The above types of studies of the birth environment of the Sun depend heavily on understanding the dynamical development of young stellar groups. In recent years much progress has been made in the understanding of general dynamics after cluster formation and the formation of low-mass clusters. However, the formation of clusters and associations with masses exceeding $1000\,M_{\odot}$ is less well understood. However, it is in such massive stellar groups where the Sun most likely formed. Any observational progress in this field of the formation of high-mass stellar groups would help to determine the solar birth cluster even better.

Here, only estimates of the long-term development of systems in the various environments were used, but future simulations should cover the entire 4.5 Gyr lifetime of the solar system. This would provide better constraints on the number of stars being ejected and SSAs being destroyed.

This could mean that there is no real difference in the likelihood in this respect between our two options, because more stars form in associations than in clusters, however, there are more low-mass than high-mass associations. Given the large uncertainties it could be equally likely that the Sun formed in any of the two remaining options.

ORCID iDs

Susanne Pfalzner https://orcid.org/0000-0002-5003-4714

References

Aarseth, S. J. 2003, Gravitational N-Body Simulations (Cambridge: Cambridge Univ. Press)
Adams, F. C. 2010, ARA&A, 48, 47
Adams, F. C., Fatuzzo, M., & Holden, L. 2014, ApJ, 789, 86
Adams, F. C., Proszkow, E. M., Fatuzzo, M., & Myers, P. C. 2006, ApJ, 641, 504
Bhandare, A., Breslau, A., & Pfalzner, S. 2016, A&A, 594, A53
Bobylev, V. V., & Bajkova, A. T. 2014, AstL, 40, 353
Boss, A. P. 2017, ApJ, 844, 113
Brasser, R., Duncan, M. J., & Levison, H. F. 2006, Icar, 184, 59
Breslau, A., Steinhausen, M., Vincke, K., & Pfalzner, S. 2014, A&A, 565, A130
Cottaar, M., Meyer, M. R., Andersen, M., & Espinoza, P. 2012, A&A, 539, A5
Cuello, N., Dipierro, G., Mentiplay, D., et al. 2019, MNRAS, 483, 4114
Dai, Y.-Z., Liu, H.-G., Wu, W.-B., et al. 2018, MNRAS, 480, 4080
Dauphas, N., & Chaussidon, M. 2011, AREPS, 39, 351
Espinoza, P., Selman, F. J., & Melnick, J. 2009, A&A, 501, 563
Fujimoto, Y., Krumholz, M. R., & Tachibana, S. 2018, MNRAS, 480, 4025
Goodson, M. D., Luebbers, I., Heitsch, F., & Frazer, C. C. 2016, MNRAS, 462, 2777
Gounelle, M. 2015, A&A, 582, A26
Hénault-Brunet, V., Evans, C. J., Sana, H., et al. 2012, A&A, 546, A73
Henney, W. J., O'Dell, C. R., Meaburn, J., Garrington, S. T., & Lopez, J. A. 2002, ApJ, 566, 315
Hester, J. J., Desch, S. J., Healy, K. R., & Leshin, L. A. 2004, Sci, 304, 1116
Ida, S., Larwood, J., & Burkert, A. 2000, ApJ, 528, 351
Jaehnig, K. O., Da Rio, N., & Tan, J. C. 2015, ApJ, 798, 126
Jílková, L., Portegies Zwart, S., Pijloo, T., & Hammer, M. 2015, MNRAS, 453, 3157
Johnstone, R. M., Fabian, A. C., & Taylor, G. B. 1998, MNRAS, 298, 854
Kenyon, S. J., & Bromley, B. C. 2004, Natur, 432, 598
Kobayashi, H., Ida, S., & Tanaka, H. 2005, Icar, 177, 246
Krause, M. G. H., Charbonnel, C., Bastian, N., & Diehl, R. 2016, A&A, 587, A53
Kroupa, P. 2002, Sci, 295, 82
Kuhn, M. A., Hillenbrand, L. A., Sills, A., Feigelson, E. D., & Getman, K. V. 2019, ApJ, 870, 32
Lada, C. J., & Lada, E. A. 2003, ARA&A, 41, 57
Lee, J.-E., Bergin, E. A., & Lyons, J. R. 2008, M&PS, 43, 1351
Li, G., & Adams, F. C. 2015, MNRAS, 448, 344
Lichtenberg, T., Parker, R. J., & Meyer, M. R. 2016, MNRAS, 462, 3979
Liu, F., Asplund, M., Yong, D., et al. 2016, MNRAS, 463, 696
Lugaro, M., Ott, U., & Kereszturi, Á. 2018, PrPNP, 102, 1
Martínez-Barbosa, C. A., Brown, A. G. A., Boekholt, T., et al. 2016, MNRAS, 457, 1062
Mitchell, T. R., & Stewart, G. R. 2011, AJ, 142, 168
Nicholson, R. B., & Parker, R. J. 2017, MNRAS, 464, 4318
O'Dell, C. R., Ferland, G. J., Henney, W. J., et al. 2015, AJ, 150, 108
O'dell, C. R., & Wen, Z. 1994, ApJ, 436, 194
Olczak, C., Kaczmarek, T., Harfst, S., Pfalzner, S., & Portegies Zwart, S. 2012, ApJ, 756, 123
Owen, J. E., Ercolano, B., Clarke, C. J., & Alexander, R. D. 2010, MNRAS, 401, 1415
Parker, R. J., Church, R. P., Davies, M. B., & Meyer, M. R. 2014, MNRAS, 437, 946
Pfalzner, S. 2004, ApJ, 602, 356
Pfalzner, S. 2009, A&A, 498, L37
Pfalzner, S. 2013, A&A, 549, A82
Pfalzner, S., Bhandare, A., & Vincke, K. 2018a, A&A, 610, A33
Pfalzner, S., Bhandare, A., Vincke, K., & Lacerda, P. 2018b, ApJ, 863, 45
Pfalzner, S., & Kaczmarek, T. 2013, A&A, 559, A38
Pfalzner, S., Umbreit, S., & Henning, T. 2005, ApJ, 629, 526
Plummer, H. C. 1911, MNRAS, 71, 460
Portegies Zwart, S. 2019, A&A, 622, A69
Portegies Zwart, S. F., & Jílková, L. 2015, MNRAS, 451, 144
Portegies Zwart, S. F., McMillan, S. L. W., & Gieles, M. 2010, ARA&A, 48, 431
Ramírez, I., Bajkova, A. T., Bobylev, V. V., et al. 2014, ApJ, 787, 154
Ricci, L., Robberto, M., & Soderblom, D. R. 2008, AJ, 136, 2136
Rochau, B., Brandner, W., Stolte, A., et al. 2010, ApJL, 716, L90
Schwamb, M. E., Brown, M. E., Rabinowitz, D. L., & Ragozzine, D. 2010, ApJ, 720, 1691
Spurzem, R., Giersz, M., Heggie, D. C., & Lin, D. N. C. 2009, ApJ, 697, 458
Steinhausen, M., & Pfalzner, S. 2014, A&A, 565, A32
Thrane, K., Bizzarro, M., & Baker, J. A. 2006, ApJL, 646, L159
Vincke, K., Breslau, A., & Pfalzner, S. 2015, A&A, 577, A115
Vincke, K., & Pfalzner, S. 2016, ApJ, 828, 48
Vincke, K., & Pfalzner, S. 2018, ApJ, 868, 1
Wang, L., Spurzem, R., Aarseth, S., et al. 2015, MNRAS, 450, 4070
Wasserburg, G. J., Busso, M., Gallino, R., & Nollett, K. M. 2006, NuPhA, 777, 5
Webb, J. J., Price-Jones, N., Bovy, J., et al. 2020, MNRAS, 494, 2268
Williams, J. P., & Gaidos, E. 2007, ApJL, 663, L33
Winter, A. J., Clarke, C. J., Rosotti, G., & Booth, R. A. 2018, MNRAS, 475, 2314
Winter, A. J., Clarke, C. J., Rosotti, G. P., Hacar, A., & Alexander, R. 2019, MNRAS, 490, 5478
Winter, A. J., Kruijssen, J. M. D., Chevance, M., Keller, B. W., & Longmore, S. N. 2020, MNRAS, 491, 903